# Boundary effects on transient radiation fields from vibrating surfaces

Daniel Guyomar and John Powers
*Department of Electrical and Computer Engineering, Naval Postgraduate School, Monterey, California 93943*

(Received 13 May 1984; accepted for publication 15 October 1984)

The transient radiation or diffraction from a planar source imbedded in an infinite baffle is analyzed for three different baffle conditions (rigid, free-space, and soft). For an excitation separable in time and space, it is shown that the field is related to the normal derivative of the input field only. A method is also given for computing the transient fields based on a wave decomposition in the spatial frequency domain. This method is a time generalization of the angular spectrum theory that presents transient wave propagation as a time-varying spatial filter, allowing a linear systems interpretation of the diffraction. The formalism is shown to easily include the effects of a finite receiving aperture. The method is amenable to computing the field from an arbitrary time excitation and an arbitrary spatial distribution. The method is valid for arbitrary distances to the observation point and uses computationally efficient FFT calculations.

PACS numbers: 43.20.Px, 43.40.At

## INTRODUCTION

Due to their limited sizes, transducers and arrays do not launch plane waves but radiate more complicated waves in accordance with diffraction phenomena. New applications of ultrasound tend to use pulsed sound more frequently than continuous radiation. Several other authors have done analyses of the diffraction of pulsed waves,[1-13] restricting their work to sources in a rigid surrounding baffle with a time-separable excitation function.

This paper addresses the problem of the effects of boundary condition assumptions on the radiated field of transducers excited with a variable spatial excitation but a uniform time excitation (i.e., the excitation signal is separable in space and time). The transducers are planar and are embedded in baffles that specify one of three boundary conditions on the field. The boundary conditions considered include: free-space, a rigid baffle, and a resilient baffle. A theoretical method is also presented for computing the time-domain impulse response and the response to an arbitrary temporal excitation in a computationally efficient form. The method is an extension of the classic angular spectrum theory. It gives a linear systems interpretation of the diffraction effects and shows how the wave propagation of an impulsively excited source can be modeled as a time-varying spatial filter that reduces the high spatial frequency content of the angular spectrum. Inversion into the space domain gives the time domain impulse response for a source with an arbitrary velocity distribution or transducer geometry. The transient response for an arbitrary time excitation is then obtained by a convolution. The use of the Fourier formalism allows incorporation of the effects of the receiving aperture as a simple multiplicative spatial filter in the spatial frequency domain. Numerical simulations are shown and a closed form solution for an important class of velocity distributions is also obtained (in the Appendix).

## I. BASIC THEORY

It is known from diffraction theory that the diffracted or radiated field, $\phi(x,y,z,t)$, can be written as

$$\phi(x,y,z,t) = \int_S \left( \phi_0 *_t \frac{\partial g}{\partial n} - g *_t \frac{\partial \phi_0}{\partial n} \right) ds, \tag{1}$$

where $\phi_0(x,y,0,t)$ is the field on the input plane (located at $z=0$), $*$ indicates the convolution operation upon the indicated variable, $n$ is the normal to the surface $S$, and $g(x,y,z,t)$ is the Green's function that solves the homogeneous wave equation as well as the assumed boundary conditions. In acoustics the quantity $\phi$ can represent the velocity potential, the $z$ velocity component, or the pressure. In the following, $\phi$ will be interpreted as the velocity potential.

The problem of finding the Green's function is solved by analyzing the reflected field of a point source over an infinite baffle. This approach is similar to Sommerfeld's ideas[14] for the impulse regime. For the three cases, the Green's function can always be written as a combination of the wave equation elementary solution, $\delta(t \pm R/c)/R$.

## II. CASE 1: FREE SPACE

When the baffle matches the properties of the propagation medium, the fields are continuous across the boundary and there is no reflection at the boundary interface. Therefore, the best-suited Green's function is the outgoing elementary solution, $\delta(t - R/c)/R$. Thus,

$$\frac{\partial}{\partial n}\left(\frac{\delta(t-R/c)}{R}\right) = \delta \frac{\partial}{\partial n}\left(\frac{1}{R}\right) - \frac{\delta'}{cR}\frac{\partial R}{\partial n}, \tag{2}$$

where $\delta'$ indicates the partial derivative of the Dirac delta function with respect to time. Substituting in Eq. (1) gives $\phi(x,y,z,t)$

$$= \int_S \left[ \tilde{\phi}_0 \frac{\partial}{\partial n}\left(\frac{1}{R}\right) - \frac{1}{cR}\frac{\partial R}{\partial n}\frac{\partial \tilde{\phi}_0}{\partial t} - \frac{1}{R}\frac{\partial \tilde{\phi}_0}{\partial n} \right] ds, \tag{3}$$

 0001-4966/85/030907-09$00.80  

where $\tilde{\phi}_0$ is the value of the function or the indicated derivative evaluated with at a retarded time, $t - R/c$. Here, we have $R = [(x-x_0)^2 + (y-y_0)^2 + (z-z_0)^2]$ with $(x,y,z)$ being the arbitrary observation position and $(x_0,y_0,z_0)$ being a point on the source plane. We will assume $z_0 = 0$. Equation (3) is the Kirchhoff formula for unsteady phenomena. We have

$$\frac{\partial R}{\partial z_0} = \frac{z_0 - z}{R}, \tag{4}$$

$$\frac{\partial}{\partial z_0}\left(\frac{1}{R}\right) = \frac{\partial}{\partial R}\left(\frac{1}{R}\right)\frac{\partial R}{\partial z_0} \tag{5}$$

$$= \frac{z - z_0}{R^3}. \tag{6}$$

For an aperture on the plane $z_0 = 0$,

$$\phi(x,y,z,t) = \int_S \left[\frac{z\tilde{\phi}_0}{R^3} + \frac{z}{cR^2}\left(\frac{\partial\tilde{\phi}_0}{\partial t}\right) - \frac{1}{R}\left(\frac{\partial\tilde{\phi}}{\partial z_0}\right)\Big|_{z_0=0}\right] ds. \tag{7}$$

For the sake of simplicity, the $x_0,y_0,z_0$ argument has been suppressed. To remove the retardation terms, we can write the last equation in the form of a convolution,

$$\phi(x,y,z,t) = \left(-\frac{\partial\phi_0}{\partial z} \underset{x}{*}\underset{y}{*} \frac{1}{R} + \phi_0 \underset{x}{*}\underset{y}{*} \frac{z}{R^3} + \frac{\partial\phi_0}{\partial t} \underset{x}{*}\underset{y}{*} \frac{z}{cR^2}\right) \underset{t}{*} \delta\left(t - \frac{R}{c}\right). \tag{8}$$

Considering Eq. (8), it is clear that the radiated potential is related to the $z$ velocity, the pressure (i.e., the time derivative of the potential), and its own value on the emitting surface. Usually the second term of the expression is dropped because of the $1/R^3$ dependence, making the expression dependent only on the velocity and the pressure. For the case of monochromatic waves, it is easy to justify this approximation and to find the bounds for propagation. For this case, at distances such that $kR \gg 1$ (where $k$ is the wavenumber), the approximation is justified. However, in the transient wave case, the assumption does not hold any longer and the potential term should be retained.

For the case where the time and space functions are separable, we can write

$$\phi_0(x,y,0,t) = \sigma(t)s(x,y). \tag{9}$$

This relation means that the surface points can vibrate with different amplitudes but with the same temporal dependence. For such a wave the wave front over the surface must be perpendicular to $z$ and must propagate along the $+z$ axis. This type of propagation causes a $t - z/c$ dependence in the expressions on the surface, consequently relating derivatives by

$$-\frac{1}{c}\frac{\partial}{\partial t} \equiv \frac{\partial}{\partial z}. \tag{10}$$

Using the relation of Eq. (10), we can relate the potential at the input plane to the velocity in that plane (since velocity information is frequently the known or assumed quantity at the input). For a velocity given by

$$v_z(x,y,0,t) = v(t)s(x,y), \tag{11}$$

the potential is given by

$$\phi_0(x,y,0,t) = cs(x,y)\int_0^t v(t')dt'. \tag{12}$$

The $z$ component of velocity in Eq. (8) is

$$-\frac{\partial\phi_0}{\partial z} = v_z \tag{13}$$

$$= \frac{1}{c}\frac{\partial\phi_0}{\partial t}. \tag{14}$$

For an impulse time excitation, we have $v(t) = \delta(t)$, and it follows that

$$\phi_0(x,y,0,t) = cH(t)s(x,y), \tag{15}$$

where $H(t)$ is the Heaviside step function. From Eq. (8) we obtain the time-domain impulse response, $\Omega(x,y,z,t)$, as

$$\Omega(x,y,z,t) = s(x,y) \underset{x}{*}\underset{y}{*} \left[\frac{\delta(t - R/c)}{R}\left(1 + \frac{z}{R}\right) + \frac{czH(t - R/c)}{R^3}\right]. \tag{16}$$

The potential for an arbitrary time excitation of velocity $v(t)$ is obtained from the results of Eq. (16) as a convolution of $v(t)$ with the time domain impulse response,

$$\phi(x,y,z,t) = v(t) \underset{t}{*} \Omega(x,y,z,t). \tag{17}$$

For both cases of Eqs. (16) and (17), the potential is related only to the vertical surface velocity. Once this velocity distribution is known, it is then possible to compute the entire field.

## III. CASE 2: PERFECTLY RIGID BOUNDARIES

For a rigid baffle the normal velocity (i.e., the normal derivative of the acoustic potential) must go to zero on the boundary. For this case the Green's function is divided into two waves: one impinging on the rigid baffle and the other is its image weighted by a reflection coefficient of 1. This Green's function is given by

$$g(x,y,z,t) = \frac{\delta\{t - [r^2 + (z-z_0)^2]^{1/2}/c\}}{[r^2 + (z-z_0)^2]^{1/2}} + \frac{\delta\{t - [r^2 + (z+z_0)^2]^{1/2}/c\}}{[r^2 + (z+z_0)^2]^{1/2}}. \tag{18}$$

For $z_0 = 0$, it follows that

$$g(x,y,z,t) = [2\delta(t - R/c)]/R \tag{19}$$

and

$$\frac{\partial g(x,y,z,t)}{\partial z} = 0. \tag{20}$$

The derivative disappears on the rigid baffle as expected. The time-domain impulse response becomes

$$\Omega(x,y,z,t) = 2s(x,y) \underset{x}{*}\underset{y}{*} [\delta(t - R/c)/R]. \tag{21}$$

## IV. CASE 3: PERFECTLY RESILIENT BOUNDARY

For a resilient boundary, the acoustic potential must be zero on the boundary. The same approach is used as in the rigid case except that the reflection coefficient is set $-1$, giving a Green's function of

$$g(x,y,z,t) = \frac{\delta\{t - [r^2 + (z - z_0)^2/c]^{1/2}\}}{[r^2 + (z - z_0)^2/c]^{1/2}} - \frac{\delta\{t - [r^2 + (z + z_0)^2/c]^{1/2}\}}{[r^2 + (z + z_0)^2/c]^{1/2}}. \quad (22)$$

At $z_0 = 0$, we obtain

$$g(x,y,z,t) = 0 \quad (23)$$

and

$$\frac{\partial g}{\partial n} = 2\left(\frac{z\delta(t - R/c)}{R^3} + \frac{z\delta'(t - R/c)}{cR^2}\right). \quad (24)$$

The time-domain impulse response for this case is

$$\Omega(x,y,z,t) = s(x,y,) \underset{x\,y}{*} \left(\frac{2z\delta(t - R/c)}{R^2} + \frac{2czH(t - R/c)}{R^3}\right). \quad (25)$$

## V. FIELD CALCULATIONS: COMPUTATIONAL TECHNIQUE

Equations (16), (21), and (25) are not easily computed directly. For the sake of computational efficiency, it is better to work in the spatial spectrum domain, $(f_x, f_y)$, where $f_x$ and $f_y$ are the spatial frequencies. To do this, we decompose the elementary solution using properties of the Dirac delta function. It should be noted that the elementary solution is a radial function. One Dirac delta function property is that,

$$\delta[f(r)] = \sum_{i=1}^{N} \delta(r - r_i) \Big/ \left|\frac{df}{dr}\right|_{r = r_i}, \quad (26)$$

where $r_i$ are the $N$ zeros of $f(r)$. After dropping the physically unrealizable term we have

$$\frac{\delta(ct - R)}{R} = \delta[r - (c^2t^2 - z^2)^{1/2}]/R\left(\frac{(c^2t^2 - z^2)^{1/2}}{ct}\right). \quad (27)$$

Taking a two-dimensional spatial transform (that then reduces to a Hankel transform due to radial symmetry), we have

$$B[\delta(ct - R)/R] = J_0[\rho(c^2t^2 - z^2)]H(t - z/c), \quad (28)$$

where $J_0$ is zero-order Bessel function and $\rho = (f_x^2 + f_y^2)^{1/2}$. Also,

$$B\left(\frac{\delta(ct - R)}{R^2}\right) = \frac{J_0[\rho(c^2t^2 - z^2)]H(t - z/c)}{ct}. \quad (29)$$

After substitution, the transform of the time-domain impulse response, $\bar{\Omega}(f_x, f_y, z, t)$, for the three cases under study can be written as

*Free space*

$$\bar{\Omega}(f_x, f_y, z, t) = \bar{s}(f_x, f_y)\left[\left(1 + \frac{z}{ct}\right)J_0[\rho(c^2t^2 - z^2)^{1/2}]H\left(t - \frac{z}{c}\right) + cH(t) \underset{t}{*} \frac{zJ_0[\rho(c^2t^2 - z^2)^{1/2}]H(t - z/c)}{c^2t^2}\right]. \quad (30)$$

*Rigid baffle*

$$\bar{\Omega}(f_x, f_y, z, t) = 2\bar{s}(f_x, f_y)\, J_0[\rho(c^2t^2 - z^2)^{1/2}]H(t - z/c). \quad (31)$$

*Resilient baffle*

$$\bar{\Omega}(f_x, f_y, z, t) = 2\bar{s}(f_x, f_y)\left[\frac{z}{ct}J_0[\rho(c^2t^2 - z^2)^{1/2}]H\left(\frac{t - z}{c}\right) + cH(t) \underset{t}{*} \frac{zJ_0[\rho(c^2t^2 - z^2)^{1/2}]H(t - z/c)}{c^2t^2}\right]. \quad (32)$$

The formulation of the last three equations is the angular spectrum theory expressed including the temporal domain. The equations link the spectrum of the radiated field to the surface information by means of a transfer function. The transfer function, $J_0[\rho(c^2t^2 - z^2)^{1/2}]$, is a time-varying one. Unlike the monochromatic case, the transfer function acts on both the magnitude and phase of the input angular spectrum. As time increases the $J_0$ function decreases, thereby enhancing the lower spatial frequencies. In the field space domain the field will become smoother as time advances due to this filtering effect.

The convolution appearing in Eqs. (30) and (32) represents an averaging of the $J_0[\rho(c^2t^2 - z^2)^{1/2}]$ term, weighted by the $1/(ct)^2$ expression. Such a convolution enhances the lower spatial spectrum components of the angular spectrum.

Since $J_0[\rho(c^2t^2 - z^2)^{1/2}] \leqslant 1$, the maximum effect of the convolution term can be estimated. Computation leads to

$$cH(t) \underset{t}{*} \frac{zJ_0[\rho(c^2t^2 - z^2)^{1/2}]}{c^2t^2} \leqslant \frac{ct - z}{ct}. \quad (33)$$

Because time must be subject to the causality constraint, we have $ct > z$. Writing $ct = z + a$ with $a > 0$, the bound becomes

$$(ct - z)/ct = a/(z + a), \quad (a > 0). \quad (34)$$

The latter relation shows that the convolution will be of less influence as the distance $z$ increases.

The effects of the type of boundary are to change the directivity factor affecting the filter function, $J_0[\rho(c^2t^2 - z^2)^{1/2}]$ and to add a second term, corresponding to a convolution for the free space and resilient baffle cases.

At time, $t = z/c$, the Bessel function will be equal to unity and the convolution vanishes. Consequently, at that point in time the field is an exact image of the source. At the same time all of the coefficients are equal and the calculated field has the same value for all three cases. This is physically seen by arguing that this field is only the waves transmitted directly from the source; the boundary influence has not been felt yet. For all cases a common feature is that the influence of the boundary condition decreases as $z$ increases.

It is interesting to note that the fields associated with a free space or resilient boundary can be written in terms of the field obtained for the the rigid baffle, $\Omega_{\text{rigid}}(x,y,z,t)$. The free-space solution is

$$\bar{\Omega}_{\text{free space}}(f_x, f_y, z, t) = \frac{\bar{\Omega}_{\text{rigid}}(f_x, f_y, z, t)}{2}\left(1 + \frac{z}{ct}\right) + cH(t) \underset{t}{*} \frac{z\bar{\Omega}_{\text{rigid}}(f_x, f_y, z, t)}{2c^2t^2}. \quad (35)$$

The solution for the resilient boundary can be written as

$$\bar{\Omega}_{\text{resilient}}(f_x,f_y,z,t) = (z/ct)\bar{\Omega}_{\text{rigid}}(f_x,f_y,z,t) + cH(t) \underset{t}{*} \frac{z\bar{\Omega}_{\text{rigid}}(f_x,f_y,z,t)}{c^2t^2}. \quad (36)$$

The inverse spatial transform of Eqs. (35) and (36) provide the fields in space. It should be noted that multiplicative terms (i.e., the directionality factors) are functions of time and have the same effect in both the space and the spatial frequency domains.

The spatial spectrum form of the solutions of Eqs. (35) and (36) are important because a closed-form solution for $\bar{\Omega}_{\text{rigid}}(f_x,f_y,z,t)$ can be found for an important class of velocity distributions. This solution is found in the Appendix.

For axisymmetric transducers, the value of $\bar{\Omega}_{\text{rigid}}(f_x,f_y,z,t)$ along the propagation axis ($r=0$) is given by

$$\Omega_{\text{rigid}}(0,z,t) = \int_0^\infty \bar{s}(\rho) J_0[\rho(c^2t^2 - z^2)^{1/2}]\rho\, d\rho \quad (37)$$

$$= s[(c^2t^2 - z^2)^{1/2}]. \quad (38)$$

The field along the propagation axis is the exact image of the velocity distribution along a radial line.

## VI. NUMERICAL SIMULATIONS

Using the spatial FFT operations produces a computation that is efficient, rapidly convergent, and independent of sampling constraints in the time domain. The computational procedure to obtain the time domain impulse response field is

(a) computation of the source angular distribution,

(b) multiplication by the spatial domain diffraction filter, $J_0[\rho(c^2t^2 - z^2)^{1/2}]$, to obtain $\bar{\Omega}_{\text{rigid}}(f_x,f_y,z,t)$ as in Eq. (31),

(c) inversion of $\bar{\Omega}_{\text{rigid}}(f_x,f_y,z,t)$ to obtain $\Omega_{\text{rigid}}(x,y,z,t)$,

(d) storage of $\Omega_{\text{rigid}}(x,y,z,t)$,

(e) multiplication by the correct directionality factor and convolution to obtain either $\Omega_{\text{free space}}(x,y,z,t)$ or $\Omega_{\text{resilient}}(x,y,z,t)$ (since the directivity factors are the same in the space domain).

For an arbitrary source distribution, the computation of the impulse response, $\Omega_{\text{rigid}}(x,y,z,t)$, for $64\times64\times50$ data points takes 24 s on an IBM 3033 mainframe computer. Once the impulse response is known, computation the field for a free-space boundary or a resilient boundary for arbitrary time excitation requires a bit more than one second of computation time. For radially symmetric fields, the two-dimensional FFTs can be replaced by a one-dimensional Hankel transform that is computationally faster.[15]

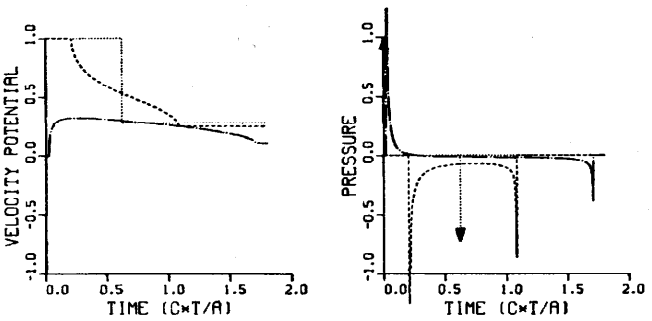


FIG. 2. Radiation patterns from a uniform circular piston imbedded in free space conditions ($z=1$ cm, $A=4$ cm). · · · · $r/A=0$; - - - - $r/A=0.25$; · - · - · - $r/A=0.57$.

Figures 1–3 show the effect of the boundary condition on the velocity potential and its time derivative (i.e., the pressure) radiated by a uniformly excited circular piston. In all of the figures, the time axis begins at the arrival time of the first wave (i.e., at $t=z/c$) and is normalized by the transducer diameter, $A=4$ cm). The sound velocity is assumed to be 1500 m/s. The dotted, dashed, and dot–dash lines represent the fields observed at $z=0.5A$ with the distance ratios of $r/A=0$, 0.25, and 0.57, respectively. The vertical arrows correspond to the derivative taken in the distributional sense with the length being proportional to the size of the discontinuity.

Figure 1 shows the field of a transducer in a rigid baffle. The results for this problem are known and cited in the literature.[1-3,10,12] The pressure on axis is reduced to two Dirac functions with opposite signs.

In the free-space case (Fig. 2), the convolution term compensates exactly for the decrease due to the directivity factor. The domains where the field was constant in the rigid case remain constant for the free space case as can be shown by the following reasoning. The convolution applied on a region of constant value will be

$$\frac{z}{c}\int_{z/c}^{t} \frac{1}{\xi^2}\, d\xi = \frac{ct-z}{ct}. \quad (39)$$

It follows immediately that

$$1 + z/ct + (ct - z)/ct = 2 \quad (40)$$

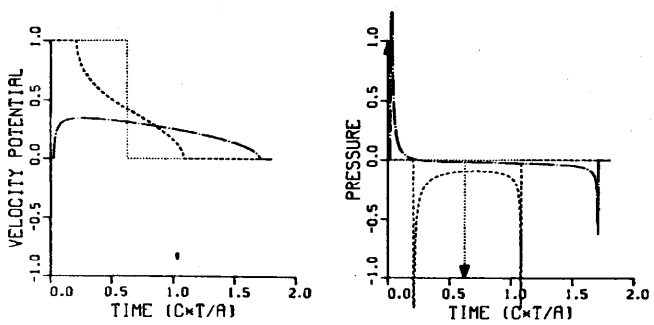


FIG. 1. Radiation patterns from a uniform circular piston imbedded in a rigid baffle ($z=1$ cm, $A=4$ cm). · · · · $r/A=0$; - - - - $r/A=0.25$; · - · - · - $r/A=0.57$.

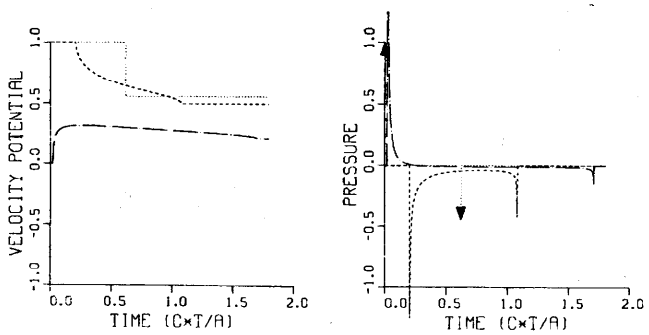


FIG. 3. Radiation patterns from a uniform circular piston imbedded in a resilient baffle ($z=1$ cm, $A=4$ cm). · · · · $r/A=0$; - - - - $r/A=0.25$; · - · - · - $r/A=0.57$.

giving a constant field for these regions. For regions of nonconstant value the potential and, consequently, the pressure undergo drastic changes. The jump discontinuity of the dotted curve (i.e., on axis) in Fig. 2 (just to the right of the 0.5 axis value) is smaller than that of Fig. 1. Off axis the slope at the other two curves of Fig. 2 is less than that of Fig. 1, thus implying a reduced pressure.

For the resilient or soft boundary case (Fig. 3), the previous calculation gives the following value in the regions of constant value,

$$2z/ct + [2(ct - z)]/ct = 2. \tag{41}$$

For the nonconstant domains, the distortion is greater than the free-space case. Due to the $2z/ct$ directivity factor the boundary influence is even greater.

The plots following Fig. 3 have been done on a $64 \times 64$ sample array. The amplitudes have been normalized to unity.

Figures 4–6 are the impulse response, observed at $z = 1$ cm, for a uniformly excited square transducer that is 2.8 cm on a side. The field is taken along a median axis. Due to the convolution, waves can exist in a region where they do not appear in the rigid baffle case. The enhancement of low frequencies induced by the convolution explains the smooth aspect of the field between the edge waves. The potential in these domains will introduce a strong radial velocity gradient responsible for the spreading of the wave. The pressure, being the time derivative of the potential, will vanish in this region.

For the nonrigid cases, as time increases further, the amplitude of the spatial spectrum will become smaller because of the time-dependent multiplicative factors. A common feature of the nonrigid boundaries is to smooth the field by enhancing the low spatial frequencies.

In Fig. 7, the field generated by the same transducer is analyzed at a distance of $z = 3$ cm. For the sake of simplicity,

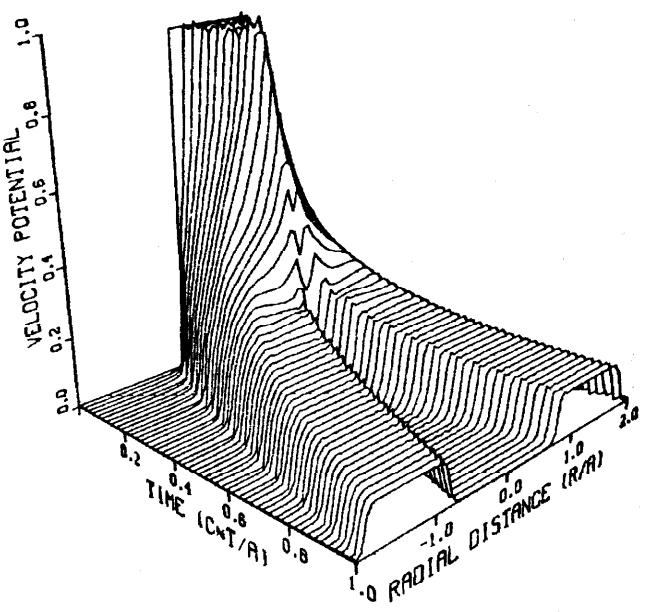


FIG. 4. Radiation pattern from a uniform square transducer imbedded in a rigid baffle ($z = 1$ cm, $A = 2.8$ cm).

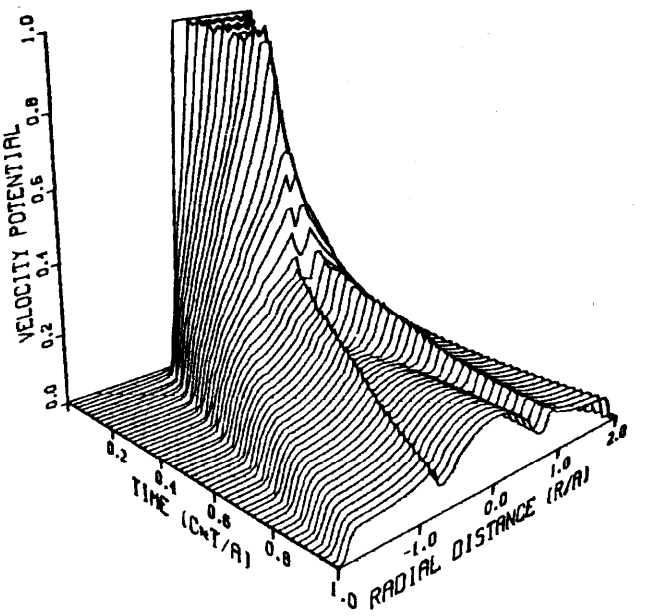


FIG. 5. Radiation pattern from a uniform square transducer imbedded in free space conditions ($z = 1$ cm, $A = 2.8$ cm).

only the resilient boundary solution is shown. The influence of the convolution term is less than it was near the transducer but it still is non-negligible.

In Fig. 8 the pattern is shown at a distance of 3 cm from a circular transducer (diam $= A = 2.8$ cm) with a Bessel velocity excitation given by

$$s(r) = J_0[2(3.83r/A)], \quad r \leqslant A. \tag{42}$$

This excitation corresponds to the first mode of a free circular membrane. The perfect similarity between the source distribution and the field along the propagation axis is clearly observed.

Figure 9 gives the impulse response field for the same circular transducer with a Gaussian spatial velocity distribu-

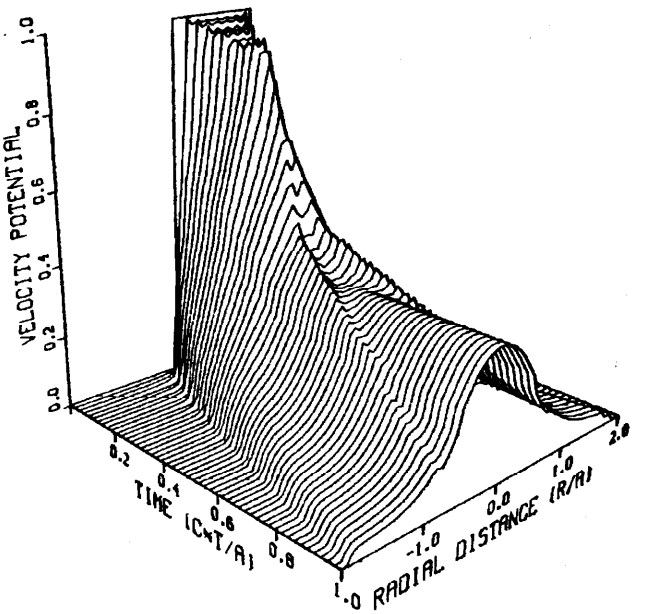


FIG. 6. Radiation pattern from a uniform square transducer imbedded in a resilient baffle ($z = 3$ cm, $A = 2.8$ cm).

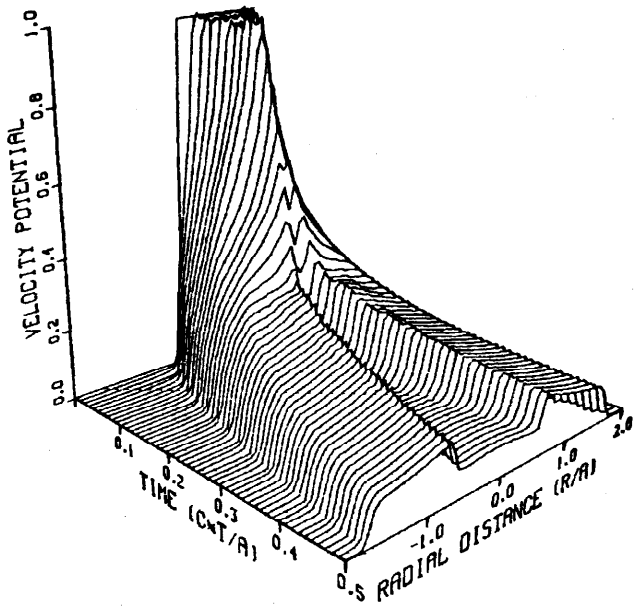


FIG. 7. Radiation pattern from a uniform square transducer imbedded in a resilient baffle ($z = 3$ cm, $A = 2.8$ cm).

tion. The $1/e$ point of the spatial excitation is at $2.8/(3)^{1/2}$ cm from the center. Because of the low spatial frequency content of the waveshape, the effect of diffraction on the beamshape is small.

## VII. ARBITRARY TIME EXCITATION

For a nonimpulse time excitation, the diffracted wave is a convolution between the impulse response and the time-varying excitation function. Figure 10 represents the transition taking place in the establishment of a monochromatic wave for a circular piston transducer. The calculations are for $z = 3$ cm. The excitation signal is a sinewave starting at $t = 0$. There are two complete cycles during the time span shown. In the plot, the modulus of the potential is shown in order to avoid obscuring the negative features of the potential. The generation of secondary lobes is clearly visible. The monochromatic behavior starts at the center and spreads out along a ray generating the secondary lobes.

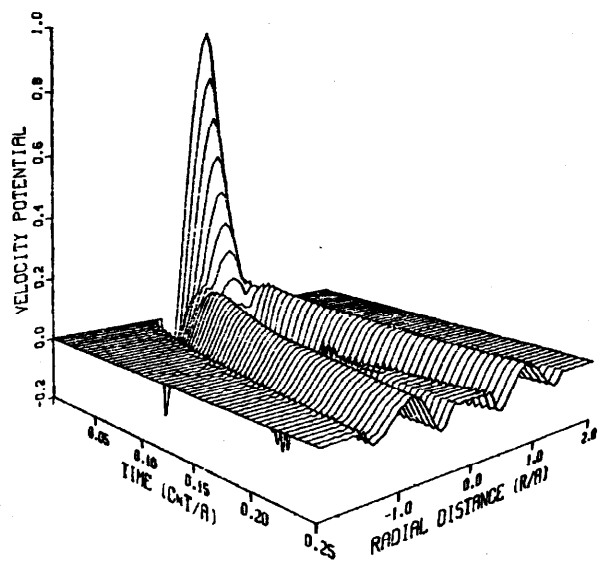


FIG. 8. Radiation from a circular transducer having a Bessel aperture function of the form, $s(r) = J_0(7.66r/A)$ ($z = 3$ cm, $A = 2.8$ cm).

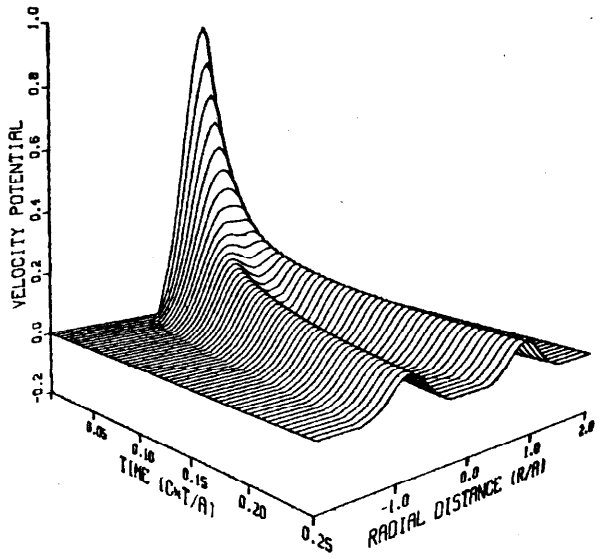


FIG. 9. Radiation from a circular transducer having a Gaussian aperture function [$1/e$ point is $A/(3)^{1/2}$ from the axis], ($z = 3$ cm, $A = 2.8$ cm).

## VIII. FINITE RECEIVER EFFECTS

A receiver with a finite aperture will perturb the observed field by averaging the wave across the aperture. The spatial frequency domain is well-suited to include this effect as the receiver contributes a low-pass filter in this domain that just multiplies the diffraction spatial filter. The averaged field can be written as

$$\langle \phi(x,y,z,t) \rangle = \int_S \phi(x - x_i, y - y_i, z, t) R(x_i, y_i) dx_i\, dy_i, \tag{43}$$

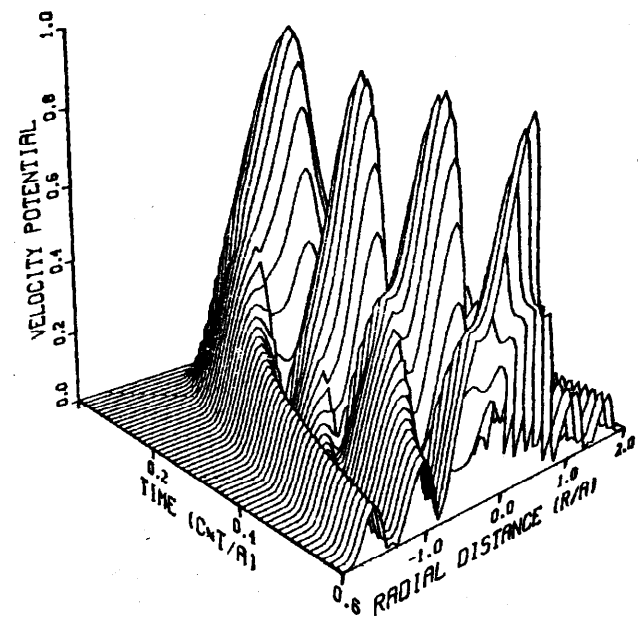


FIG. 10. Transition into a monochromatic wave ($z = 3$ cm, $A = 2.8$ cm).

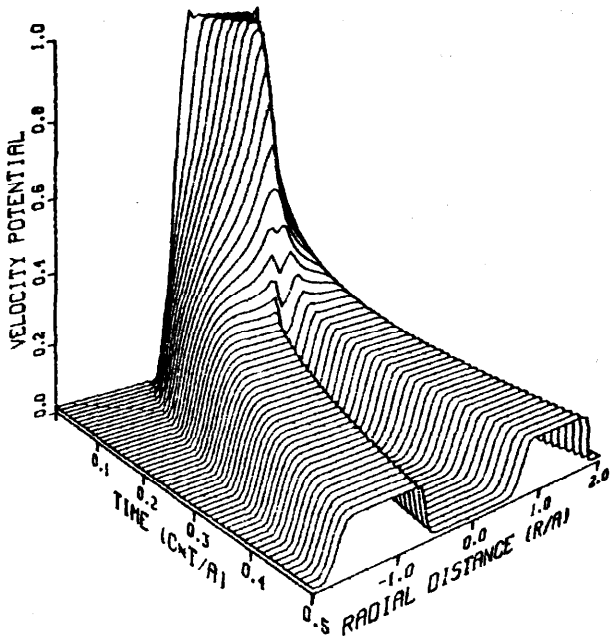


FIG. 11. Impulse response of a square transducer ($z = 3$ cm, $A = 2.8$ cm) measured with a finite-size circular receiver (radius = 2 mm).

where $R(x_i, y_i)$ is the aperture function over the surface $S$. The spatial convolution becomes a product in the spatial frequency domain. Hence the effective transducer function of propagation and reception will be $\overline{R}(f_x, f_y) \times J_0[\rho(c^2t^2 - z^2)^{1/2}]$.

In Figs. 11 and 12 the source is a uniformly vibrating square and the receiver is a circular transducer of radius $a = 2$ mm and $a = 5$ mm, respectively. The smoothing introduced by the averaging process is evident in both plots.

## IX. SUMMARY

Exact solutions of the radiated field have been given in the three cases: rigid baffle, free space, and a soft or resilient baffle. The influence of a term that is frequently dropped, [i.e., the second term on the right side of Eq. (8)], has been emphasized and the maximum effects of the convolution have been found in Eq. (34).

A Fourier space approach has been developed leading to a time-varying filter interpretation of the wave propagation. The main features of this filter is to enhance the lower spatial frequencies as time progresses by reducing the contributions of the higher spatial frequencies. Hence, the propagation process can be modeled as a low-pass filter having a "bandwidth" that decreases as time progresses. The method does not require any sampling constraints allowing any sampling required by the user. The method provides the temporal impulse response and through convolution, the response to a general time excitation.

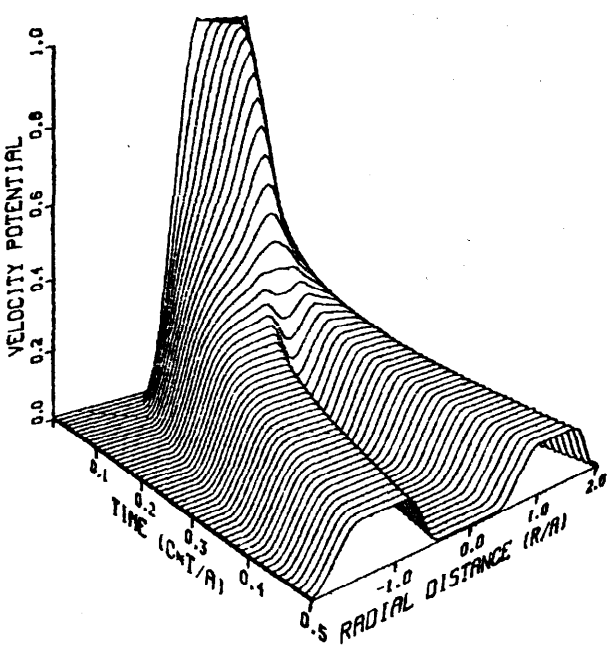


FIG. 12. Impulse response of a square transducer ($z = 3$ cm, $A = 2.8$ cm) measured with a finite-size circular receiver (radius = 5 mm).

## ACKNOWLEDGMENTS

This research was partially supported by the Foundation Research program of the Naval Postgraduate School. Daniel Guyomar is research associate of the National Research Council.

## APPENDIX

The spatial frequency formulation allows us to find a closed-form solution for an important set of velocity distributions. Each element of this set is written as

$$s(r) = \begin{cases} A(a^2 - r^2)^{\mu}, & r < a, \\ 0, & r > a, \end{cases} \tag{A1}$$

where $\mu$ is restricted to real values greater than $-1$. The case of $\mu = 0$ is a uniform piston transducer; $\mu = 1$ is a simply supported transducer, and $\mu = 2$ is a damped transducer. This set of excitations represents a wide class of velocity distributions.

The Hankel transform of Eq. (A1) has a standard form given by[16]

$$\bar{s}(\rho) = 2^{\mu}\Gamma(\mu + 1)a^{\mu+1}[J_{\mu+1}(\rho a)/\rho^{\mu+1}], \tag{A2}$$

where $\Gamma(x)$ is the gamma function. Substituting this expression into Eq. (31) and taking the inverse transform gives

$$\Omega_{\text{rigid}}(r,z,t) = 2^{\mu}\Gamma(\mu + 1)a^{\mu+1}\int_0^{\infty} \frac{J_{\mu+1}(\rho a)}{\rho^{\mu+1}} \times J_0[\rho(c^2t^2 - z^2)^{1/2}]J_0(\rho r)\rho\, d\rho. \tag{A3}$$

The latter integral is evaluated with the Sonine–Dougall formula

$$\int_0^{\infty} J_{\omega}(\alpha t)J_{\xi}(\beta t)J_{\xi}(\gamma t)t^{1-\omega}\, dt = \frac{2^{-\omega+1+\xi}(\beta\gamma)^{\xi}}{\alpha^{\omega}\Gamma(\omega - \xi)\Gamma(\xi + 1/2)\Gamma(1/2)} \times \int_0^{A} (\alpha^2 - \beta^2 - \gamma^2 + 2\beta\gamma\cos\eta)^{\omega-\xi-1}\sin^{2\xi}\eta\, d\eta, \tag{A4}$$

with

$$A=\begin{cases}0, & \text{for } \alpha^2<(\beta-\gamma)^2,\\ \cos^{-1}\left(\dfrac{\beta^2+\gamma^2-\alpha^2}{2\beta\gamma}\right), & \text{for } (\beta-\gamma)^2<\alpha^2<(\beta^2+\gamma^2),\\ \pi, & \text{for } (\beta+\alpha)^2<\alpha^2.\end{cases} \tag{A5}$$

Substituting these results into Eq. (A4) leads to

$$\Omega(r,z,t)=\frac{1}{\pi}\int_0^A(\Delta+\sigma\cos\eta)^\mu\,d\eta, \tag{A6}$$

where

$$\Delta=a^2-c^2t^2+z^2-r^2 \tag{A7}$$

and

$$\sigma=2r(c^2t^2-z^2)^{1/2}. \tag{A8}$$

The solution to Eq. (A6) exists for real values of $\mu$.[17] However, the solution involves complicated functions in the form of Legendre functions, hence they will not be cited in this paper, since we seek only solutions that are easily implemented on a computer. For integer values of $\mu$, the integral evaluations have simpler form

$$\Omega(r,z,t)=\frac{\sigma^\mu}{\pi}\int_0^A\left(\frac{\Delta}{\sigma}+\cos\eta\right)^\mu d\eta \tag{A9}$$

$$=\frac{\sigma^\mu}{\pi}\sum_{k=0}^{\mu}\binom{\mu}{k}\left(\frac{\Delta}{\sigma}\right)^{\mu-k}\int_0^A\cos^k\eta\,d\eta \tag{A10}$$

$$=\frac{\sigma^\mu}{\pi}\left[\sum_{k=0}^{\tau_1}\binom{\mu}{2k}\left(\frac{\Delta}{\sigma}\right)^{\mu-2k}\int_0^A\cos^{2k}\eta\,d\eta+\sum_{k=0}^{\tau_2}\binom{\mu}{2k+1}\left(\frac{\Delta}{\sigma}\right)^{\mu-2k-1}\int_0^A\cos^{2k+1}\eta\,d\eta\right], \tag{A11}$$

where

$$\tau_1=\mu/2, \quad \text{if } \mu \text{ even}, \tag{A12}$$

$$\tau_2=\mu/2-1, \tag{A13}$$

and

$$\tau_1=\mathrm{Int}[\mu/2], \quad \text{if } \mu \text{ odd}, \tag{A14}$$

$$\tau_2=\mathrm{Int}[\mu/2], \tag{A15}$$

where Int[ ] is the operator that returns the integer part of the argument. The notation in Eq. (A11) is

$$\binom{\mu}{k}\equiv\frac{\mu!}{k!(\mu-k)!}. \tag{A16}$$

The integrals in Eq. (A11) are known.[17] Using the notation

$$E_{2k}(A)\equiv\int_0^A\cos^{2k}\eta\,d\eta \tag{A17}$$

$$=\frac{1}{2^{2k}}\binom{2k}{k}A+\frac{1}{2^{2k-1}}\sum_{1=0}^{k-1}\binom{2k}{1}\frac{\sin(2k-21)A}{2k-21}, \tag{A18}$$

$$E_{2k+1}(A)\equiv\int_0^A\cos^{2k+1}\eta\,d\eta \tag{A19}$$

$$=\frac{1}{2^{2k}}\sum_{1=0}^{k}\binom{2k+1}{1}\frac{\sin(2k-21+1)A}{2k-21+1}. \tag{A20}$$

It follows from a few manipulations that, (1) for $r<a$ (i.e., inside the disk boundary)

$$\Omega(r,z,t)=\begin{cases}\sigma^\mu\displaystyle\sum_{k=0}^{\tau_1}\binom{\mu}{2k}\left(\frac{\Delta}{\sigma}\right)^{\mu-2k}\frac{1}{2^{2k}}\binom{2k}{k}, & \text{for } z<ct<[z^2+(a-r)^2]^{1/2},\\ \dfrac{\sigma^\mu}{\pi}\left[\displaystyle\sum_{k=0}^{\tau_1}\binom{\mu}{2k}\left(\frac{\Delta}{\sigma}\right)^{\mu-2k}E_{2k}(A)+\sum_{k=0}^{\tau_2}\binom{\mu}{2k+1}\left(\frac{\Delta}{\sigma}\right)^{\mu-2k-1}E_{2k+1}(A)\right], & \\ \quad \text{for } [z^2+(a-r)^2]^{1/2}<ct<[z^2+(a+r)^2]^{1/2}, & \\ 0, \quad \text{for } ct>[z^2+(a+r)^2]^{1/2}: & \end{cases} \tag{A21}$$

(2) for $r>a$ (i.e., outside the boundary of the disk)

$$\Omega(r,z,t)=\begin{cases}0, \quad \text{for } z<ct<[z^2+(a-r)^2]^{1/2},\\ \dfrac{\sigma^\mu}{\pi}\left[\displaystyle\sum_{k=0}^{\tau_1}\binom{\mu}{2k}\left(\frac{\Delta}{\sigma}\right)^{\mu-2k}E_{2k}(A)+\sum_{k=0}^{\tau_2}\binom{\mu}{2k+1}\left(\frac{\Delta}{\sigma}\right)^{\mu-2k-1}E_{2k+1}(A)\right], & \\ \quad \text{for } [z^2+(a-r)^2]^{1/2}<ct<[z^2+(a+r)^2]^{1/2}, & \\ 0, \quad \text{for } ct>[z^2+(a+r)^2]^{1/2}. & \end{cases}$$

It can be shown that for $\mu=0$, the preceding reduces to the known solution for a circular piston transducer. The results mentioned earlier apply to a certain class of velocity distributions. It should be noted that all combinations within the described set of velocity distributions will have a closed form solution, thereby increasing the range of possible distributions.


[1]F. Oberhettinger, "On transient solutions of the baffled piston problem," J. Res. Natl. Bur. Stand. **65B**, 1–6 (1961).

[2]G. E. Tupholme, "Generation of acoustic pulses by baffled plane pistons," Mathematika **16**, 209–224 (1969).

[3]P. R. Stepanishen, "Transient radiation from pistons in an infinite planar baffle," J. Acoust. Soc. Am. **49**, 1629–1637 (1971).

[4]P. R. Stepanishen, "Experimental verification of the impulse response method to evaluate transient acoustic fields," J. Acoust. Soc. Am. **63**, 1610–1617 (1981).

[5]G. R. Harris, "Review of transient field theory for a baffled planar piston," J. Acoust. Soc. Am. **70**, 10–20 (1981).

[6]G. R. Harris, "Transient field of a baffled piston having an arbitrary vibration amplitude distribution," J. Acoust. Soc. Am. **70**, 186–204 (1981).

[7]J. Weight and A. Hayman, "Observation of the propagation of very short

ultrasonic pulses and their reflection by small targets," J. Acoust. Soc. Am. **63**, 396–404 (1978).
[8]J. A. Archer-Hall, A. I. Bashter, and A. J. Hazelwood, "A means for computing the Kirchoff surface integral for a disk radiator as a single integral with fixed limits," J. Acoust. Soc. Am. **65**, 1568–1570 (1979).
[9]M. Fink, "Theoretical study of pulsed echocardiographic focusing procedures," in *Acoustical Imaging*, edited by P. Alais and A. Metherell (Plenum, New York, 1980), Vol. 10, pp. 437–453.
[10]D. Guyomar and J. Powers, "Diffraction of pulsed ultrasonic waves in lossless and absorbing media," submitted to IEEE Trans. Sonics Ultrason.
[11]M. Pappalardo, N. Deninsenko, G. Scarano, and M. Matteucci, "Description of the pulsed acoustic field of a linear diagnostic ultrasound array using a simple approximated expression," presented at Acoustical Imaging, '83, Minneapolis, October 1983 (to be published in *Acoustical Imaging*, Vol. 13, Plenum, New York).
[12]P. W. Buchen and R. A. W. Haddon, "Diffraction of a plane pulse by thin arbitrarily shaped obstacles," J. Acoust. Soc. Am. **68**, 309–313 (1980).
[13]D. Guyomar and J. Powers, "Transient fields radiated by curved surfaces-application to focusing," submitted for publication.
[14]J. W. Goodman, *Introduction to Fourier Optics* (McGraw-Hill, New York, 1968).
[15]S. Candel, "An algorithm for the Fourier–Bessel transform," Comput. Phys. Commun. **23**, 343–353 (1981).
[16]A. Erdelyi, W. Magnus, F. Oberhettinger, and F. G. Triconi, *Tables of Integral Transforms*, Vol. 2 (McGraw-Hill, New York, 1954), p. 52.
[17]I. S. Gradshteyn and I. Ryzhik, *Table of Integrals, Series and Products* (Academic, New York, 1965).